

# Contrastive Learning of Global and Local Audio-Visual Representations

Shuang Ma<sup>1</sup> Zhaoyang Zeng<sup>2</sup> Daniel McDuff<sup>1</sup> Yale Song<sup>1</sup>

## Abstract

Contrastive learning has delivered impressive results in many audio-visual representation learning scenarios. However, existing approaches optimize for learning either *global* representations useful for tasks such as classification, or *local* representations useful for tasks such as audio-visual source localization and separation. While they produce satisfactory results in their intended downstream scenarios, they often fail to generalize to tasks that they were not originally designed for. In this work, we propose a versatile self-supervised approach to learn audio-visual representations that generalize to both the tasks which require global semantic information (e.g., classification) and the tasks that require fine-grained spatio-temporal information (e.g. localization). We achieve this by optimizing two cross-modal contrastive objectives that together encourage our model to learn discriminative global-local visual information given audio signals. To show that our approach learns generalizable video representations, we evaluate it on various downstream scenarios including action/sound classification, lip reading, deepfake detection, and sound source localization.

## 1. Introduction

Contrastive self-supervised learning (CSL) aims to learn representations that generalize to a variety of downstream tasks (Oord et al., 2018; Hjelm et al., 2018; He et al., 2020; Chen et al., 2020). In CSL, the choice of “contrasting views” plays a crucial role because the learned representations capture information shared between different views (Bachman et al., 2019). Recently, Tian et al. (2020) have shown that the optimal choice of views depends critically on the downstream scenario. This requires a careful design of the contrastive objectives depending on the intended downstream tasks; consequently, existing works focus on finding opti-

<sup>1</sup>Microsoft Research, Redmond, WA, USA <sup>2</sup>Sun Yat-sen University, Guangzhou, China. Correspondence to: Shuang Ma <shuama@microsoft.com>.

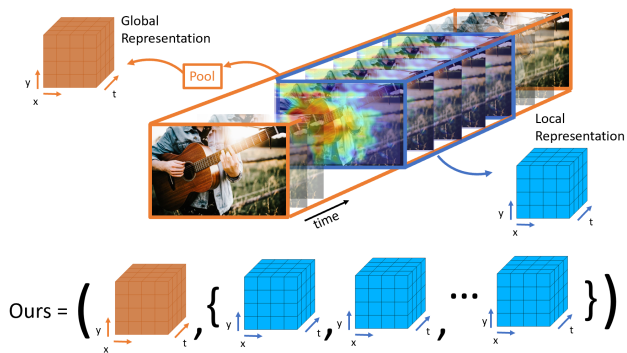


Figure 1. While many self-supervised approaches optimize for high-level *or* low-level tasks, we present an approach to learn both global *and* local representations from video.

mal views tailored for the intended downstream tasks. For example, Hjelm & Bachman (2020) extend DIM (Hjelm et al., 2018) to the spatio-temporal domain by assuming that information useful for action classification, i.e. global semantics, should be invariant across space and time within a given video. When dealing with multimodal data, Morgado et al. (2020) learns from audio-visual correspondence in videos, assuming that information needed for audio/video classification should be shared between the two modalities.

Although existing approaches achieve impressive results in their intended downstream tasks, they often fail to generalize to tasks that they were not originally designed for, e.g., global representations for tasks that require local information. For example, as we show in our experiments, global representations learned via CSL (e.g., by contrasting clip-level embeddings from different time steps of the same video) do not generalize well to the lipreading task (Chung & Zisserman, 2016), which requires fine-grained *local* spatio-temporal representations around the mouth region.

The progress made so far provides important insights for learning scenario-specific (global or local) representations, but we argue that the current paradigm of designing CSL approaches specific to the intended downstream scenarios is not ideal. It not only limits the generalizability of the learned representations, evaluating the approaches solely on the intended scenarios could produce misleading conclusions.

Motivated by this, in this paper we take an orthogonal di-

rection to the current CSL approaches and aim to learn representations agnostic to the types of downstream scenarios. Specifically, we propose a versatile CSL approach that learns representations generalizable to both the scenarios that require global representations (e.g., classification) and scenarios that require local representations (e.g., localization). We then demonstrate that representations learned by our approach successfully transfer to both the “global” and “local” tasks without having to re-pretrain the model with different objectives, thus improving the generalizability of the learned representations.

Our approach, which we call *global-local cross-modal* (GLCM) contrastive learning, builds on the recent advances in CSL that leverage audio-visual correspondence as the primary learning signal (Owens et al., 2016; Korbar et al., 2018). To learn global and local representations, we define two cross-modal contrastive objectives defined at different temporal granularities (see Fig. 1). A visual sequence with a low sampling rate constructs a global view, while one with a high sampling rate constitutes a local view. We contrast the views only at the matching granularities, i.e., global-to-global and local-to-local. We encourage the global views to capture *slowly changing* information by using samples from different videos as negatives, and the local views to capture *time-varying* information by using samples from different time regions of the same video as negatives. Furthermore, we encourage the views to also capture fine-grained spatial information by forming contrasting views at the grid level rather than at the frame level. As a result, we obtain global-local spatio-temporal representations that exhibit strong audio-visual correlations.

We evaluate our GLCM pretraining approach by transferring the learned representations to downstream tasks that need local spatio-temporal information (i.e. lip reading, deep-fake detection, and sound-source localization) and also discriminative tasks that needs global information (i.e. action classification and audio-event classification). Most importantly, we show that the same pretrained model can successfully transfer to all our scenarios. To the best of our knowledge, our work is the first to demonstrate a self-supervised approach that learns representations generalizable to both global and local video understanding scenarios.

## 2. Related Work

**Contrastive self-supervised learning.** Contrastive learning leverage multiple views of the same data (Oord et al., 2018), e.g., multiple perspectives within the same modality such as augmentations of the same image, different frames of a video, etc. (He et al., 2020; Hjelm & Bachman, 2020; Han et al., 2019a) or perspectives from different modalities such as depth and RGB images, visual and textual signals (Tian et al., 2019; Sun et al., 2019; Miech et al.,

2020; Alayrac et al., 2020). Chen et al. (2020) and Hjelm et al. (2018) show that leveraging local information to perform contrastive learning further improves performance on image classification. DIM (Hjelm et al., 2018) has been extended to multi-scale (Bachman et al., 2019) and video data (Hjelm & Bachman, 2020). However, evaluation is still focused on “discriminative” tasks, e.g., image classification and video event classification, while there is little evidence that these models will adapt well to the local information.

**Audio-visual representation learning.** Several approaches leverage correspondence between audio and visual signals for CSL (Asano et al., 2020; Korbar et al., 2018; Alwassel et al., 2019; Morgado et al., 2020; Patrick et al., 2020; Chung et al., 2019). Most existing approaches aim to capture high-level semantic information from observations. It has been empirically demonstrated that such learned information is very effective for “discrimination tasks” (classification). However, in tasks that needs local information, representations learn by such approaches may not perform well. Xiao et al. (2020a) utilize different temporal scales of the audio and visual data, which encourages the model to capture fine-grained temporal information. However, their evaluation was limited to classification tasks. In contrast with previous work, we demonstrate that our approach effectively learns global-local audio-visual representations by evaluating on a variety of downstream tasks.

## 3. Approach

We use audio and visual channels of video data as cross-modal views and utilize the same visual sequence processed at different sampling rates to learn representations at different granularities. To encourage each signal to capture complementary views of the same data, we use different encoders to extract representations from audio and visual sequences, i.e., we define an audio encoder  $E_a$  and two visual encoders  $E_v^g$  (global) and  $E_v^l$  (local) that handle visual sequences sampled at different granularities.

To learn global and local representations we define two cross-modal contrastive objectives. The global objective is defined over visual sequences with a low sampling rate (Sec.3.1), while the local objective is defined over visual sequences with a high sampling rate (Sec.3.2). To jointly train our model with the global and local objectives, we propose a spatially-aware attention pooling mechanism to effectively reuse fine-grained spatial information captured from the global encoder for learning the local encoder (Sec.3.3).

### 3.1. Global Contrastive Objective

We design the global contrastive objective to capture slowly changing information with high audio-visual correlation. We use visual sequences captured at low sampling rates,

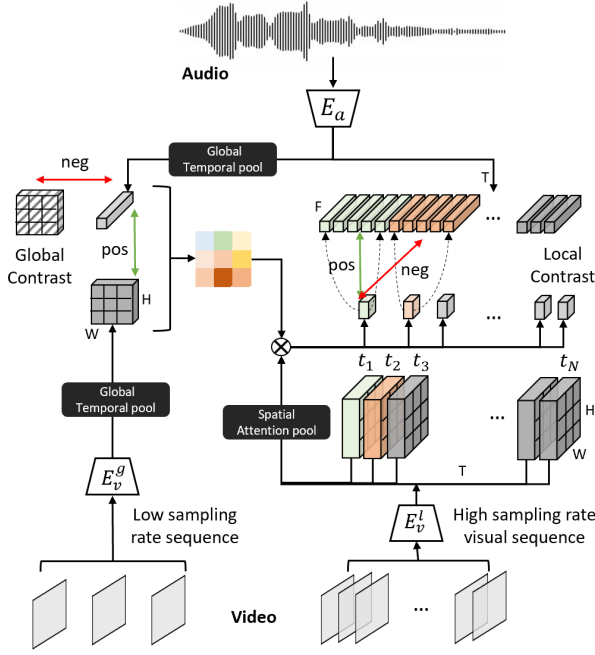


Figure 2. Our GLCM architecture. For clarity we omit the channel dimension and show only the spatial and temporal dimensions. In the “global contrast” part (the left half), visual features are shown with different shading patterns (e.g., diagonal-hatch, filled gray) and indicate those that come from different video samples. In the “local contrast” part (the right half), we use colors to indicate different time windows.

which will purposely lack local temporal information.

$E_a$  encodes an audio sequence into an audio embedding  $z_a \in \mathbb{R}^{T \times F}$ , where  $T$  is the sequence length and  $F$  is the number of frequency bands. We perform global temporal pooling and obtain  $z_a \in \mathbb{R}^{1 \times F}$ . Similarly, we perform global temporal pooling on features encoded by the global visual encoder  $E_v^g$ , which produces global visual embedding  $z_v^g \in \mathbb{R}^{1 \times H \times W \times C}$ . For the visual features, we preserve spatial information by performing global pooling only along the temporal dimension.

To compute the global contrastive loss, we consider audio features  $z_a$  and visual features  $z_v^g$  that come from the same video sample as positive pairs, while features coming from different video samples are negative pairs. To encourage our model to also capture local *spatial* information in  $z_v^g$ , we consider each cell of the  $H \times W$  spatial grid as an instance and define pairs by coupling  $z_a$  with  $z_v^g[i]$ ,  $i \in H \times W$ . Note that not all  $z_v^g[i]$  will have valid audio-visual correspondence to  $z_a$ ; it is rather likely that only a few cell (e.g., the lip region of a talking person) will match the information in  $z_a$ . To resolve this misalignment issue, we adopt MIL-

NCE (Miech et al., 2020) to define our global loss  $\mathcal{L}_g$ :

$$-\log \left( \frac{\sum_{z_v^g[i] \in \mathcal{P}} F(z_a, z_v^g[i])}{\sum_{z_v^g[i] \in \mathcal{P}} F(z_a, z_v^g[i]) + \sum_{z' \in \mathcal{N}} F(z'_a, z_v^{lg})} \right)$$

where  $F(z_a, z_v) = \exp(z_a^T z_v)$  measures the compatibility between audio and visual samples,  $\mathcal{P}$  is a set of spatial grids in  $z_v^g$ , and  $\mathcal{N}$  is a set of negative visual samples taken from different videos, i.e., given a batch of  $B$  videos and a spatial grid of  $H \times W$  in visual features, we consider  $H \times W \times (B - 1)^2$  negative pairs.

### 3.2. Local Contrastive Objective

We design the local contrastive objective to capture fine-grained spatio-temporal information sensitive to temporal changes, e.g., the lip region of a talking head. Unlike the global objective, we take a temporally-granular approach and contrast local views per time step to capture information in a local temporal neighborhood.

We obtain audio features  $z_a$  by using the same audio encoder  $E_a$  but without global temporal pooling. The local visual features  $z_v^l$  are obtained by feeding the visual sequence with a high sampling rate into the local visual encoder  $E_v^l$ , which produces the visual features  $z_v^l \in \mathbb{R}^{T \times H \times W \times C}$ . We then perform spatial pooling to obtain  $z_v^l \in \mathbb{R}^{T \times 1 \times 1 \times C}$ .

To obtain representations sensitive to temporal changes, we take an audio sequence and the corresponding visual sequence from the same local temporal block as positives; we then take visual sequences from different blocks of the same video as negatives. We illustrate this in Fig. 2: Audio and visual features shaded in the same color refer to those in the same temporal block, while those in different temporal blocks (e.g. green and orange blocks) are considered as negative pairs. This encourages the shared information between modalities to be just how features vary over time.

Note that a single visual slice maps to multiple audio slices because audio signals are typically captured at a higher sampling rate. As we illustrate in Fig. 2, one visual slice  $z_v^l[t]$  (green block) corresponds to  $M$  audio slices  $z_a[t_k]$ ,  $t_k \in M$  (five green blocks). To model this one-to-many relationship we again use MIL-NCE (Miech et al., 2020) to define the local contrastive loss  $\mathcal{L}_l$ :

$$-\log \left( \frac{\sum_{z_a[t_k] \in \mathcal{P}} F(z_a[t_k], z_v^l[t])}{\sum_{z_a[t_k] \in \mathcal{P}} F(z_a[t_k], z_v^l[t]) + \sum_{z' \in \mathcal{N}} F(z'_a, z_v^l)} \right)$$

where  $\mathcal{P}$  is a set of audio slices that correspond to  $z_v^l[t]$  and  $\mathcal{N}$  is a set of all possible audio-visual slice pairs that come from different parts of the same video (we do not consider slices from different videos as negatives), i.e., given a video with  $T$  visual slices and  $M \times T$  audio slices, we consider  $M \times (T - 1)^2$  negative pairs.

### 3.3. Spatially-Aware Attention Pooling

As discussed in Sec. 3.1, the global contrastive objective captures not only slowly changing temporal information but also local spatial information. Intuitively, the dot product between  $z_a$  and  $z_v^g[i]$ ,  $i \in H \times W$  can be seen as a spatial attention map indicating the regions of high audio-visual correlation. For example, in a video of someone talking, the lip region will have a relatively higher score than the background, and in a video of someone playing a guitar, finger regions will have high scores (see Fig. 3).

We can utilize the spatial attention maps to perform spatial pooling on the visual features used in the local contrastive objective. Specifically, for a local visual feature  $z_v^l[t]$  we use the attention map computed from  $z_a$  and  $z_v^g$  to perform spatial pooling. Compared to average or max pooling, the attention-pooled features give more weight to regions with high audio-visual correspondence, thus improving the efficacy of the local contrastive objective. We demonstrate the effectiveness of spatial attention pooling in Table 1 and 2.

## 4. Experiments

**Implementation details.** We use 3D-ResNet18 (Hara et al., 2018) for our visual encoders ( $E_v^g$  and  $E_v^l$ ) and 1D-ResNet18 for our audio encoder, in both cases using Batch Normalization (BN) (Ioffe & Szegedy, 2015). All models are trained end-to-end with the ADAM optimizer (Kingma & Ba, 2014) with an initial learning rate  $\gamma = 10^{-3}$  after a warm-up period of 500 iterations. We use 16 NVIDIA Tesla P100 GPUs with a batch size of 32 for our experiments.

During self-supervised pretraining, we preprocess video frames by sampling at 10 FPS and applying random cropping, horizontal flipping, gray-scaling, and temporal jittering. We resize video frames to three-channel images of  $112 \times 112$ ; we set the clip length to 32 frames for the local visual encoder, and to 8 frames for the global visual encoder. From the audio channel we extract mel-spectrograms from the raw waveform using the LibROSA library and get a  $80 \times T$  matrix with 80 frequency bands;  $T$  is proportional to the length of an audio clip. We then segment the mel-spectrogram according to the corresponding video clips to ensure temporal alignment. We treat the mel-spectrograms as an 80-channel 1D signal. For downstream tasks we follow the standard data preprocessing protocols.

For the global contrastive loss we use features at a  $16 \times 16$  spatial resolution. To compute the local contrastive loss, we adopt a temporal window of size three without overlap.

**Datasets.** Many audio and visual downstream tasks of interest involve human actions (e.g., audio and video classification), faces (e.g., deepfake detection), and speech (e.g., lip reading). Therefore, we use a combination of Kinetics-

700 (Carreira et al., 2019) and AVSpeech (Ephrat et al., 2018) for pretraining. Specifically, we randomly select 120K video samples from each datasets, which gives us a dataset of 240K samples; we term it as K-AV. For comparison with the other state-of-the-art approaches, we pretrain our model on the K-AV dataset, which is at the same scale as the Kinetics-700 dataset. For the ablation study, we pretrain our model on a subset of 15K samples from the K-AV dataset, we term as K-AV-15K.

We evaluate our pretrained models on several downstream tasks: on action recognition using UCF101 (Soomro et al., 2012) and HMDB51 (Kuehne et al., 2011), and on sound classification using ESC50 (Piczak, 2015b). For lip reading, we evaluate our model on both LRW (Chung & Zisserman, 2016) and LRS2 (Chung et al., 2017). For deepfake detection, we evaluate our model on a subset of DFDC (Dolhansky et al., 2019).

### 4.1. Downstream Scenarios

**Lip Reading.** Visually recognizing a speaker’s utterance is useful and challenging task. For example, lip movements for different sounding letters can be visually similar to each other (e.g., b and p, d and t). This requires the learned visual representation to contain fine-grained spatio-temporal information, rather than global semantics. In evaluating our pretrained model on the lip reading task, we focus on investigating whether our approach successfully learns fine-grained spatio-temporal visual information. For a fair comparison with state-of-the-art (SOTA) approaches, we use the same data processing protocol as Zhang et al. (2019). For LRW and LRS2, we detect 68 facial landmarks in each video frame using dlib (Castelli & Pagano, 2002). We use the outer eye and nose tip landmarks to align the detected face in each frame using an affine transform. Finally, an image of size  $112 \times 112$  is cropped from the aligned face with the lip landmarks at the center. The cropping is applied such that the lip region occupies one third of the image width. During finetuning, we apply random horizontal flipping. We concatenate the global features and local features produced by our pretrained  $E_v^g$  and  $E_v^l$ , respectively. Both encoders are finetuned with the whole model.

In Table 1 we compare our approach with SOTA supervised and self-supervised lip reading methods. For LRW, we evaluate on a 500-way word classification task and report top-1 accuracy. For LRS, we report the word error rate (WER). The results show that our approach outperforms SOTA supervised approaches on both LRS and LRW by a large margin, i.e. 4.7% WER reduction on LRS and 5.1% accuracy improvements on LRW, and outperforms SOTA self-supervised approaches with the same backbone and using the same pretraining dataset. These results show that our proposed approach can capture the fine-grained spatio-

Training	Model	Backbone	Dataset	LRS↓	LRW↑
Supervised	LRW (Chung & Zisserman, 2016)	VGG-M	LRW	-	61.10
	Res. (Stafylakis & Tzimiropoulos, 2017)	ResNet34	LRW	-	83.00
	TwoStream (Weng & Kitani, 2019)	I3D	LRW	-	84.07
	DFTN (Xiao et al., 2020b)	ResNet18	LRW500, 1000	-	<u>84.1</u>
	Perfect Match (Chung et al., 2019)	TC-5	LRW	71.6	-
	TM-CTC (Afouras et al., 2018)	ResNet	LRS2-BBC	65	-
	TM-sep2seq (Afouras et al., 2018)	ResNet	LRS2-BBC	<u>49.8</u>	-
	WAS (Chung et al., 2017)	Conv.		70.4	76.2
	STF (Zhang et al., 2019)	ResNet18	LRW, LRS2,3	51.7	83.7
Self-supervised	MoCo (He et al., 2020)	ResNet18	K-AV-15K	71.5	61.2
	CPC (Oord et al., 2018)	ResNet18	K-AV-15K	66.7	65.3
	DPC (Oord et al., 2018)	ResNet18	K-AV-15K	65.1	67.5
	InfoMax (Hjelm & Bachman, 2020)	ResNet18	K-AV-15K	<u>53.2</u>	70.7
	AVSlowFast (Xiao et al., 2020a)	ResNet18	K-AV-15K	56.1	<u>75.8</u>
	Ours	ResNet18	LRS2, 3	46.7	86.9
		ResNet18	K-AV-15K	<u>47.8</u>	<u>83.7</u>
		ResNet18	K-AV-240K	<b>45.1</b>	<b>89.2</b>

Table 1. Comparison with SOTA on lipreading: LRS (WER, lower is better) and LRW (top-1 accuracy). Underline are the best results from the supervised approaches. Blue text highlights the comparison of ours with the self-supervised approaches under the same setting.

temporal information necessary for lip reading.

**Deepfake Detection.** We hypothesis that “deepfakes” tend to be characterized by audio-visual inconsistencies such as a misalignment between lip motions and audio, unnatural facial and lip appearance/movements or asymmetry between facial regions such as the left and right eyes. Such artifacts could be detected through local spatio-temporal features.

We take our pretrained model and finetune it on 1 second segments from the DFDC dataset (Dolhansky et al., 2019) for 100 epochs with a batch size of 16. We evaluate performance using video-wise Area Under the Curve (AUC). We follow the same data preprocessing protocol as in SOTA approaches for this task, and use the same training and test video sets as Chugh et al. (2020). We perform face detection to crop the face region in each video frame. We concatenate the global and local visual features that are produced by our pretrained global and local visual encoders, and finetune the pretrained encoders with the whole model.

Table 2 shows the results. Among all the compared approaches, Chugh et al. (2020) and Mittal et al. (2020) use both visual and audio sequences, while the other approaches use only the visual sequences for detection. As we can see, when using only visual signal, our approach outperforms all previous SOTA approaches (AUC=96.7). We also compare our model with the other SOTA self-supervised approaches (shown in blue color). Again, our model outperform the best benchmark by a large margin (90.1 vs. 85.3).

**Action and Sound Classification.** To demonstrate our model learning discriminative global representations, we evaluate our approach on action and sound classification. For action classification, we finetune both pretrained global and local visual encoders by concatenating the global and lo-

cal representations. For audio classification, we finetune our pretrained audio encoder  $E_a$  with the audio classification model. To evaluate on action and audio classification, we compare both our models that were pretrained on Kinetics-700 and K-AV-240K with SOTA approaches pretrained on a dataset of the same scale (Kinetics). We find that on all three benchmarks, i.e. UCF101, HMDB51 and ESC50, our approach achieves a new SOTA (91.2% on UCF101, 61.9% on HMDB51 and 80.1% on ESC50) - see Table 3.

## 4.2. Ablation and analysis

**The importance of global-local contrasts for tasks requiring local information.** We investigate how pretext tasks impact local information needed for downstream tasks (i.e., lip reading and deepfake detection) and compare our task with those used in other work. We pretrain our model and the other SOTA self-supervised approaches with the same backbone (3DResNet-18) and the pretraining dataset (K-AV-15K). After pretraining, we finetune each model on the downstream benchmarks following the same protocol.

Table 4 shows that, when we vary only the pretext task during pretraining, our models outperform all the baselines by a large margin, which demonstrates the effectiveness of our proposed approach. We also find that InfoMax and AVSlowFast outperform the others (MoCo, DPC and CPC). We believe this is because InfoMax draws more attention to the spatial local information and AVSlowFast learns more fine-grained temporal information, which are critical for the tasks of lip reading and deepfake detection. MoCo, which is successful for visual classification tasks, fails in both lip reading and deepfake detection. This supports our argument that using the “vallina” CSL may not achieve good performance for a large variety of different tasks.

Contrastive Learning of Global and Local Audio-Visual Representations

Training	Model	Visual	Audio	Backbone	AUC $\uparrow$
Supervised	Capsule (Nguyen et al., 2019b)	✓		VGG-19	53.3
	Multi-task (Nguyen et al., 2019a)	✓		Y-shape	53.6
	HeadPose (Yang et al., 2019)	✓		-	55.9
	Two-stream (Zhou et al., 2017)	✓		Inception3	61.4
	VA-MLP (Matern et al., 2019)	✓		-	61.9
	VA-LogReg (Matern et al., 2019)	✓		-	66.2
	Meso4 (Afchar et al., 2018)	✓		Inception4	75.3
	Xception-c40 (Rossler et al., 2019)	✓		Xception	69.7
	Xception-c23 (Rossler et al., 2019)	✓		Xception	72.2
	FWA (Li & Lyu, 2018)	✓		-	72.7
	DSP-FWA (Li & Lyu, 2018)	✓		-	75.5
	Siamese (Mittal et al., 2020)	✓	✓	-	84.4
	MDS (Chugh et al., 2020)	✓	✓	ResNet18	<u>91.5</u>
Self-supervised	MoCo (He et al., 2020)	✓		ResNet18	60.2
	CPC (Oord et al., 2018)	✓		ResNet18	67.9
	DPC (Han et al., 2019b)	✓		ResNet18	71.2
	InfoMax (Hjelm & Bachman, 2020)	✓		ResNet18	<u>85.3</u>
	AVSlowFast (Xiao et al., 2020a)	✓		ResNet18	80.9
	Unimodal (DFDC)	✓		ResNet18	95.5
	Multimodal (DFDC)	✓	✓	ResNet18	95.6
	Ours (K-AV-15K)	✓		ResNet18	<u>90.1</u>
	Ours (K-AV-240K)	✓		ResNet18	<b>96.7</b>

Table 2. Comparison with SOTA approaches on deepfake detection. For training on DFDC, we use the same training and test splits as (Chugh et al., 2020). Mittal et al. (2020) use the same number of randomly sampled training data (180K). All the numbers of the other SOTA approaches are collected from (Chugh et al., 2020). All the self-supervised approaches are pretrained on K-AV-15K, and finetuned and tested on the same training and test sets of DFDC.

	Method	Pretrain Dataset	UCF101 $\uparrow$	HMDB51 $\uparrow$	ESC50 $\uparrow$
Supervised	Scratch	-	46.5	17.1	-
	Scratch Random Forest (Piczak, 2015b)	-	-	-	44.3
	Scratch ConvNet (Piczak, 2015a)	-	-	-	64.5
	Scratch ConvRBM (Sailor et al., 2017)	-	-	-	86.5
	Supervised	ImageNet	82.8	46.7	-
Self-supervised	RotNet3D (Jing & Tian, 2018)	K400 240K	62.9	33.7	-
	AVTS (Korbar et al., 2018)	K400 240K	85.8	56.9	76.7
	MotionPred (Wang et al., 2019)	K400 240K	61.2	33.4	-
	ST-Puzzle (Kim et al., 2019)	K400 240K	65.8	33.7	-
	ClipOrder (Xu et al., 2019)	K400 240K	72.4	30.9	-
	CBT (Sun et al., 2019)	K400 240K	79.5	44.6	-
	DPC (Han et al., 2019a)	K400 240K	75.7	35.7	-
	XDC (Alwassel et al., 2019)	K400 240K	84.2	47.1	78.0
	SeLaVi (Asano et al., 2020)	K400 240K	83.1	47.1	-
	AVID (Morgado et al., 2020)	K400 240K	87.5	60.8	<u>79.1</u>
	GDT (Patrick et al., 2020)	K400	<u>89.3</u>	60.0	-
	Ours	K700 240K	<b>91.2</b>	<b>61.9</b>	79.7
		K-AV 240K	90.1	61.3	<b>80.1</b>

Table 3. Comparison of SOTA approaches on action classification and sound classification. We specify pretraining dataset and the number of samples used if they are reported in the original papers (-: not available). We highlight the **best** results and the second best results.

**The role of global and local information.** To demonstrate the importance of jointly learning global-local representations during pretraining, we evaluate a baseline model that was pretrained without the local contrastive objective (Ours w/o local cont.). Table 5 shows that, when compared with the model which was pretrained using our full objective (Ours), the performance significantly drops on all the benchmarks. Optimizing only for global representations during

pretraining generalizes poorly to the tasks that require local information. Note that, for a fair comparison, we use only the global features (Global Feat.) for each downstream tasks. Furthermore, we test whether using the local, global, or both global and local features after pretraining yields better performance. We can see that, the best performance is achieved by utilizing both the global and local features and this is true for all the benchmarks. For comparison, we

Model	Pretext task	LRS↓	LRW↑	DFDC↑
MoCo (He et al., 2020)	Moment. Cont.	71.5	61.2	60.2
CPC (Oord et al., 2018)	Pred. Cont.	66.7	65.3	67.9
DPC (Han et al., 2019b)	Dense Pred. Cont.	65.1	67.5	71.2
InfoMax (Hjelm & Bachman, 2020)	Glo-loc NCE	<u>53.2</u>	70.7	<u>85.3</u>
AVTS (Korbar et al., 2018)	AVS	72.1	64.9	63.1
AVSlowFast (Xiao et al., 2020a)	AVS + Rot	56.1	75.8	80.9
Ours	Glo-loc MIL	<b>47.8</b>	<b>83.7</b>	<b>90.1</b>

Table 4. Comparison with existing self-supervised pretraining approaches on lip reading and deepfake detection. All the results are computed based on the implementation by us. We pretrain each SOTA model with the same pretext task proposed in their paper. “Moment. Cont.”: momentum contrast; “Pred. Cont.”: predictive contrast; “Dense. Pred. Cont.”: dense predictive contrast; “Glo-loc NCE”: global-local NCE; “AVS”: audio-visual sync; “Rot”: rotation detection

report the results achieved by the other SOTA approaches when using both the global and local features.

**The role of MIL-NCE in local contrastive objective.** In our local contrastive objective, we adopt the MIL-NCE as our loss function. Mieh et al. (2020) also employed the MIL-NCE as the loss function to mitigate the misalignment of visual and text signals in narrated videos. Different from their motivation, our goal here is to encourage fine-grained temporal alignment of the audio with visual features. To validate its effectiveness, we evaluate an alternative without MIL-NCE as the local contrastive loss function. Specifically, we adopt an average temporal pooling on each window of the audio features and use the vanilla contrastive loss (Chen et al., 2020) over the synchronized audio and visual features. The results are shown in Table 6. As we can see, when we perform the local contrast without the MIL-NCE objective, the performance on lip reading and deepfake detection drops considerably. While for activity classification, both loss function achieves comparable results.

**The role of spatial attention.** We leverage the global contrastive objective to capture local spatial information and use it as an attention map to assist local representation learning. Intuitively, our attention maps measure the amount of audio-visual correlation; such attention maps can highlight discriminative face regions useful for lip reading. We demonstrate the quality of our attention maps by replacing lip bounding boxes typically used in lip reading with our attention map. Specifically, instead of extracting features from the cropped lip/face region, we extract features from the entire frame (no lip/face cropping) and use our attention map to pool the features spatially. Note that the purpose of this experiment is to evaluate the quality of attention maps; we use audio signal just to obtain attention maps and discard it for word classification/deepfake detection.

The results (“Ours Attention”) show that it achieves results comparable to our best setting. On LRW and DFDC, it even outperforms SOTA approaches without relying on lip/face region detectors (which require substantial supervision on their own). It indicates that using global and local infor-

mation in a collaborative way can yield good performance. In the lip reading task, local spatial information makes the local contrast objective pay more attention to lip movement, and thus achieves comparable effects of using a lip region detector. We also evaluate our model which finetuned directly on full frames. As we can see, when discarding the localized region obtained either by detectors or by attention mechanism, the performance significantly drops on all three benchmarks. It further validates the critical role of the attention mechanism in our approach.

**Interpretation of the learned representation.** To investigate how well local spatial information is captured through the global audio-visual contrastive objective, we visualize the attention maps induced by the pretrained audio and global video encoders. Such visualization can also be considered as performing sound source localization, i.e. locate objects that making sound. To achieve this goal, the network should capture the audio-visual correlation in a spatio-temporal grid. We thus use the attention map obtained by our pretrained model to visualize the sounding source in each frame. To investigate further, we use the Kinetics-Sounds (Carreira et al., 2019) dataset as videos in the dataset generally have a high-level of audio-visual correspondence. Specifically, we add another softmax layer on the obtained attention map, and then do bilinear interpolation of the  $16 \times 16$  attention map back to the original image size, i.e.  $192 \times 192$ .

Fig. 3 shows that our learned attention maps successfully localize sounding sources in videos. Especially, when visual content is highly related to the corresponding audio signal, our model performs particularly well. For example, the first row (frames from “playing instruments” videos) shows that our model can localize the sounding region. For other activities like “baby talking,” “playing basketball,” “running,” our model highlights regions with humans. We find that the attention map incorrectly highlights regions on samples that have ambiguous audio-visual relation. We show failure cases in the last two frames of the third row. As we can see, there is no visual content that clearly relates with the audio signal, and thus the model fails to find sounding sources.

## Contrastive Learning of Global and Local Audio-Visual Representations

Model	Feature	LRS↓	LRW↑	DFDC↑	UCF101↑	HMDB51↑
w/o loc.	Glob.	70.9	65.3	67.9	82.3	57.1
Ours	Glob.	47.6 (↓ 23.3)	86.8 (↑ 21.5)	92.6 (↑ 24.7)	89.2 (↑ 6.9)	59.9 (↑ 2.8)
Ours	Loc.	46.5	88.9	95.9	88.5	58.3
Ours	Glob.+Loc.	<b>45.1</b>	<b>89.2</b>	<b>96.7</b>	<b>90.1</b>	<b>61.3</b>

Table 5. The roles of global and local information on different benchmarks. “Ours”: our model that pretrained with the whole objective. “Ours w/o loc.”: our model that pretrained without the local contrastive objective. “Glob.”: features extracted from the global encoder. “Loc.”: features extracted from the local encoder. Underline refers to the best results from the other approaches.

Local Contrastive	LRS↓	LRW↑	DFDC↑	UCF101↑	HMDB51↑
w/o MIL	40.4	79.2	88.9	87.8	56.3
Ours	47.8(↑ 7.4)	83.7(↑ 4.5)	90.1(↑ 1.2)	88.1(↑ 0.3)	56.8(↑ 0.5)

Table 6. Comparison of models pretrained with and without using MIL for local contrast.

Benchmark	SOTA	Our Best	Ours Full frame	Ours Attention
LRS↓	49.8 TM-seq2seq	45.1	71.9	51.2 (No lip crop)
LRW↑	84.1 DFTN	89.2	62.3	85.1 (No lip crop)
DFDC↑	85.3 InfoMax V 91.5 MDS V+A	96.7 V 97.1 V+A	68.1 V –	95.9 (No face crop)

Table 7. Evaluation on the role of attention mechanism in our approach. “V” uses only visual sequence and “V+A” uses both visual and audio sequence for finetuning on downstream tasks.



Figure 3. Visualization of attention maps showing the audio-visual correlations in learned representations.

## 5. Conclusion

We presented a contrastive self-supervised approach to learning global and local audio-visual representations. Using audio and low-sampled and high-sampled video sequences as separate “views” of the data, we find that learned representations generalize well to tasks involving global semantic un-

derstanding and fine-grained spatio-temporal understanding. We perform experiments on lip reading, deepfake detection, sound source localization, and action/sound classification tasks and in each case achieve strong results.

## References

- Afchar, D., Nozick, V., Yamagishi, J., and Echizen, I. Mesonet: a compact facial video forgery detection network. In *2018 IEEE International Workshop on Information Forensics and Security (WIFS)*, pp. 1–7. IEEE, 2018.
- Afouras, T., Chung, J. S., Senior, A., Vinyals, O., and Zisserman, A. Deep audio-visual speech recognition. *IEEE Transactions on Pattern Analysis and Machine Intelligence*, pp. 1–1, 2018.
- Alayrac, J.-B., Recasens, A., Schneider, R., Arandjelović, R., Ramapuram, J., De Fauw, J., Smaira, L., Dieleman, S., and Zisserman, A. Self-supervised multimodal versatile networks. *Advances in Neural Information Processing Systems*, 33, 2020.
- Alwassel, H., Mahajan, D., Torresani, L., Ghanem, B., and Tran, D. Self-supervised learning by cross-modal audio-video clustering. *arXiv preprint arXiv:1911.12667*, 2019.
- Asano, Y. M., Patrick, M., Rupprecht, C., and Vedaldi, A. Labelling unlabelled videos from scratch with multimodal self-supervision. *arXiv preprint arXiv:2006.13662*, 2020.
- Bachman, P., Hjelm, R. D., and Buchwalter, W. Learning representations by maximizing mutual information across views. In *Advances in Neural Information Processing Systems*, pp. 15535–15545, 2019.
- Carreira, J., Noland, E., Hillier, C., and Zisserman, A. A short note on the kinetics-700 human action dataset. *arXiv preprint arXiv:1907.06987*, 2019.
- Castelli, D. and Pagano, P. Opendlib: A digital library service system. In Agosti, M. and Thanos, C. (eds.), *Research and Advanced Technology for Digital Libraries*, pp. 292–308, Berlin, Heidelberg, 2002. Springer Berlin Heidelberg.
- Chen, T., Kornblith, S., Norouzi, M., and Hinton, G. A simple framework for contrastive learning of visual representations. *arXiv preprint arXiv:2002.05709*, 2020.
- Chugh, K., Gupta, P., Dhall, A., and Subramanian, R. Not made for each other-audio-visual dissonance-based deepfake detection and localization. *arXiv preprint arXiv:2005.14405*, 2020.
- Chung, J. S. and Zisserman, A. Lip reading in the wild. In *Asian Conference on Computer Vision*, 2016.
- Chung, J. S., Senior, A., Vinyals, O., and Zisserman, A. Lip reading sentences in the wild. In *2017 IEEE Conference on Computer Vision and Pattern Recognition (CVPR)*, pp. 3444–3453. IEEE, 2017.
- Chung, S.-W., Chung, J. S., and Kang, H.-G. Perfect match: Improved cross-modal embeddings for audio-visual synchronisation. In *ICASSP 2019-2019 IEEE International Conference on Acoustics, Speech and Signal Processing (ICASSP)*, pp. 3965–3969. IEEE, 2019.
- Dolhansky, B., Howes, R., Pflaum, B., Baram, N., and Ferrer, C. C. The deepfake detection challenge (dfdc) preview dataset. *arXiv preprint arXiv:1910.08854*, 2019.
- Ephrat, A., Mosseri, I., Lang, O., Dekel, T., Wilson, K., Hassidim, A., Freeman, W. T., and Rubinstein, M. Looking to listen at the cocktail party: A speaker-independent audio-visual model for speech separation. *arXiv preprint arXiv:1804.03619*, 2018.
- Han, T., Xie, W., and Zisserman, A. Video representation learning by dense predictive coding. In *ICCV*, 2019a.
- Han, T., Xie, W., and Zisserman, A. Video representation learning by dense predictive coding. In *Proceedings of the IEEE International Conference on Computer Vision Workshops*, pp. 0–0, 2019b.
- Hara, K., Kataoka, H., and Satoh, Y. Can spatiotemporal 3d cnns retrace the history of 2d cnns and imagenet? In *CVPR*, 2018.
- He, K., Fan, H., Wu, Y., Xie, S., and Girshick, R. Momentum contrast for unsupervised visual representation learning. In *Proceedings of the IEEE/CVF Conference on Computer Vision and Pattern Recognition*, pp. 9729–9738, 2020.
- Hjelm, R. D. and Bachman, P. Representation learning with video deep infomax. *arXiv preprint arXiv:2007.13278*, 2020.
- Hjelm, R. D., Fedorov, A., Lavoie-Marchildon, S., Grewal, K., Bachman, P., Trischler, A., and Bengio, Y. Learning deep representations by mutual information estimation and maximization. *arXiv preprint arXiv:1808.06670*, 2018.
- Ioffe, S. and Szegedy, C. Batch normalization: Accelerating deep network training by reducing internal covariate shift. *arXiv preprint arXiv:1502.03167*, 2015.
- Jing, L. and Tian, Y. Self-supervised spatiotemporal feature learning by video geometric transformations. *arXiv preprint arXiv:1811.11387*, 2018.
- Kim, D., Cho, D., and Kweon, I. S. Self-supervised video representation learning with space-time cubic puzzles. In *AAAI*, 2019.
- Kingma, D. P. and Ba, J. Adam: A method for stochastic optimization. *arXiv preprint arXiv:1412.6980*, 2014.

- Korbar, B., Tran, D., and Torresani, L. Cooperative learning of audio and video models from self-supervised synchronization. In *Advances in Neural Information Processing Systems*, 2018.
- Kuehne, H., Jhuang, H., Garrote, E., Poggio, T., and Serre, T. Hmdb: a large video database for human motion recognition. In *ICCV*, 2011.
- Li, Y. and Lyu, S. Exposing deepfake videos by detecting face warping artifacts. *arXiv preprint arXiv:1811.00656*, 2018.
- Matern, F., Riess, C., and Stamminger, M. Exploiting visual artifacts to expose deepfakes and face manipulations. In *2019 IEEE Winter Applications of Computer Vision Workshops (WACVW)*, pp. 83–92, 2019.
- Miech, A., Alayrac, J., Smaira, L., Laptev, I., Sivic, J., and Zisserman, A. End-to-end learning of visual representations from uncurated instructional videos. In *2020 IEEE/CVF Conference on Computer Vision and Pattern Recognition (CVPR)*, pp. 9876–9886, Los Alamitos, CA, USA, jun 2020. IEEE Computer Society. doi: 10.1109/CVPR42600.2020.00990. URL <https://doi.ieeecomputersociety.org/10.1109/CVPR42600.2020.00990>.
- Mittal, T., Bhattacharya, U., Chandra, R., Bera, A., and Manocha, D. Emotions don’t lie: An audio-visual deepfake detection method using affective cues. In *Proceedings of the 28th ACM International Conference on Multimedia*, pp. 2823–2832, 2020.
- Morgado, P., Vasconcelos, N., and Misra, I. Audio-visual instance discrimination with cross-modal agreement. *arXiv preprint arXiv:2004.12943*, 2020.
- Nguyen, H. H., Fang, F., Yamagishi, J., and Echizen, I. Multi-task learning for detecting and segmenting manipulated facial images and videos. *arXiv preprint arXiv:1906.06876*, 2019a.
- Nguyen, H. H., Yamagishi, J., and Echizen, I. Capsule-forensics: Using capsule networks to detect forged images and videos. In *ICASSP 2019-2019 IEEE International Conference on Acoustics, Speech and Signal Processing (ICASSP)*, pp. 2307–2311. IEEE, 2019b.
- Oord, A. v. d., Li, Y., and Vinyals, O. Representation learning with contrastive predictive coding. *arXiv preprint arXiv:1807.03748*, 2018.
- Owens, A., Wu, J., McDermott, J. H., Freeman, W. T., and Torralba, A. Ambient sound provides supervision for visual learning. In *European conference on computer vision*, pp. 801–816. Springer, 2016.
- Patrick, M., Asano, Y. M., Fong, R., Henriques, J. F., Zweig, G., and Vedaldi, A. Multi-modal self-supervision from generalized data transformations. *arXiv preprint arXiv:2003.04298*, 2020.
- Piczak, K. J. Environmental sound classification with convolutional neural networks. In *International Workshop on Machine Learning for Signal Processing (MLSP)*, 2015a.
- Piczak, K. J. ESC: Dataset for environmental sound classification. In *Proceedings of the 23rd ACM international conference on Multimedia*, 2015b.
- Rossler, A., Cozzolino, D., Verdoliva, L., Riess, C., Thies, J., and Nießner, M. Faceforensics++: Learning to detect manipulated facial images. In *Proceedings of the IEEE International Conference on Computer Vision*, pp. 1–11, 2019.
- Sailor, H. B., Agrawal, D. M., and Patil, H. A. Unsupervised filterbank learning using convolutional restricted boltzmann machine for environmental sound classification. In *INTERSPEECH*, 2017.
- Soomro, K., Zamir, A. R., and Shah, M. Ucf101: A dataset of 101 human actions classes from videos in the wild. *arXiv preprint arXiv:1212.0402*, 2012.
- Stafylakis, T. and Tzimiropoulos, G. Combining residual networks with lstms for lipreading. *arXiv preprint arXiv:1703.04105*, 2017.
- Sun, C., Baradel, F., Murphy, K., and Schmid, C. Contrastive bidirectional transformer for temporal representation learning. *arXiv preprint arXiv:1906.05743*, 2019.
- Tian, Y., Krishnan, D., and Isola, P. Contrastive multiview coding. *arXiv preprint arXiv:1906.05849*, 2019.
- Tian, Y., Sun, C., Poole, B., Krishnan, D., Schmid, C., and Isola, P. What makes for good views for contrastive learning. *arXiv preprint arXiv:2005.10243*, 2020.
- Wang, J., Jiao, J., Bao, L., He, S., Liu, Y., and Liu, W. Self-supervised spatio-temporal representation learning for videos by predicting motion and appearance statistics. In *CVPR*, 2019.
- Weng, X. and Kitani, K. Learning spatio-temporal features with two-stream deep 3d cnns for lipreading. *arXiv preprint arXiv:1905.02540*, 2019.
- Xiao, F., Lee, Y. J., Grauman, K., Malik, J., and Feichtenhofer, C. Audiovisual slowfast networks for video recognition. *arXiv preprint arXiv:2001.08740*, 2020a.
- Xiao, J., Yang, S., Zhang, Y., Shan, S., and Chen, X. Deformation flow based two-stream network for lip reading. *arXiv preprint arXiv:2003.05709*, 2020b.

- Xu, D., Xiao, J., Zhao, Z., Shao, J., Xie, D., and Zhuang, Y. Self-supervised spatiotemporal learning via video clip order prediction. In *CVPR*, 2019.
- Yang, X., Li, Y., and Lyu, S. Exposing deep fakes using inconsistent head poses. In *ICASSP 2019-2019 IEEE International Conference on Acoustics, Speech and Signal Processing (ICASSP)*, pp. 8261–8265. IEEE, 2019.
- Zhang, X., Cheng, F., and Wang, S. Spatio-temporal fusion based convolutional sequence learning for lip reading. In *Proceedings of the IEEE/CVF International Conference on Computer Vision (ICCV)*, October 2019.
- Zhou, P., Han, X., Morariu, V. I., and Davis, L. S. Two-stream neural networks for tampered face detection. In *2017 IEEE Conference on Computer Vision and Pattern Recognition Workshops (CVPRW)*, pp. 1831–1839. IEEE, 2017.